GEOLOGY | THE GEOLOGICAL SOCIETY OF AMERICA®

https://doi.org/10.1130/G45105.1

Manuscript received 1 May 2018
Revised manuscript received 2 July 2018
Manuscript accepted 30 July 2018

Published online 30 August 2018

Seesaw pattern in dust accumulation on the Chinese Loess Plateau forced by late glacial shifts in the East Asian monsoon

Zhiwei Xu[1]*, Thomas Stevens[2], Shuangwen Yi[1], Joseph A. Mason[3], and Huayu Lu[1]
[1]School of Geography and Ocean Science, Nanjing University, Nanjing 210023, China
[2]Department of Earth Sciences, Uppsala University, Uppsala 75236, Sweden
[3]Department of Geography, University of Wisconsin–Madison, Madison, Wisconsin 53706, USA

ABSTRACT

Recent chronological studies have revealed significant site-specific variations in loess sedimentation, which challenge the use of loess deposits as continuous, easily analyzable paleoclimate and dust records. However, the regional comparability of loess sedimentation at subglacial-interglacial time scales has not yet been systematically tested. This study focused on the spatial and temporal variability of loess sedimentation on the Chinese Loess Plateau (CLP) during the last 20 thousand years and found a clear seesaw pattern across the CLP, indicated by rapid dust accumulation at the desert margin and reduced accumulation/less preservation on the main part of the CLP after ca. 15 ka. This spatial inhomogeneity of loess sedimentation at millennial time scales is controlled by various dust transportation, trapping, and postdepositional processes in different geographic settings, which are ultimately attributed to a combined effect of a weakened winter monsoon and enhanced summer monsoon after the termination of Heinrich event 1.

INTRODUCTION

Loess deposits on the Chinese Loess Plateau (CLP) are valuable terrestrial archives that have been widely investigated to understand past dust and monsoon dynamics (Liu and Ding, 1998). Recent advances in luminescence dating allow precise determination of the age of the loess and have challenged the view that the loess is a continuous, undisturbed paleoclimate record (Lu et al., 2006; Stevens et al., 2006, 2018). High-sampling-resolution luminescence studies at individual loess sites in the CLP (e.g., Sun et al., 2012; Kang et al., 2013; Stevens et al., 2016) suggest that dust deposition is episodic at millennial time scales. In some cases, rapid changes in dust accumulation can be linked to abrupt changes in the monsoon climate (Sun et al., 2012; Újvári et al., 2017), while in other cases, rapid monsoon signals recorded in loess may be obscured by pedogenesis or other site-specific influences on accumulation and/or preservation (Stevens et al., 2008; Sun et al., 2010).

These recent findings and the variability of results leave many open questions about the fundamental nature of the loess record and its interpretation as a monsoon and dust archive. Whether episodic dust deposition or postdepositional alteration at individual sites exhibits regional synchronicity at subglacial-interglacial time scales has not been tested. Furthermore, one intriguing possibility raised recently has been the idea that glacial loess is being eroded on the desert margin of the CLP, in a process of eolian cannibalism of preexisting loess deposits (Kapp et al., 2015; Licht et al., 2016). While recent high-resolution infrared stimulated luminescence (IRSL) dating of samples from the past 250 k.y. at the desert marginal CLP site at Jingbian showed substantial gaps in the preserved sediment record (Stevens et al., 2018), supporting this eolian cannibalism hypothesis, full testing of this theory requires detailed understanding of patterns in loess deposition and preservation across the whole CLP. Better understanding of patterns in loess sedimentation processes over a large geographical area is required to determine the degree of integrity of the loess record and the extent to which variations in millennial-scale climate and dust activity are recorded (Schaetzl et al., 2018). To address these issues, we investigated the variability and regional comparability of loess sedimentation on the CLP during the past 20 k.y., focusing on subglacial-interglacial time scales.

SETTING AND METHODS

Three new sites (LP03, LP12, and LP19) from the transition zone of the northern CLP and the Mu Us dune field were investigated (Fig. 1). Loess in this transition zone is often interbedded with eolian sand. A detailed chronology of the new sites was established by quartz optically stimulated luminescence (OSL) dating techniques. Grain size in the sections was analyzed with a Malvern 2000G laser diffraction particle analyzer after removal of organic matter and carbonate. For OSL dating, purified quartz

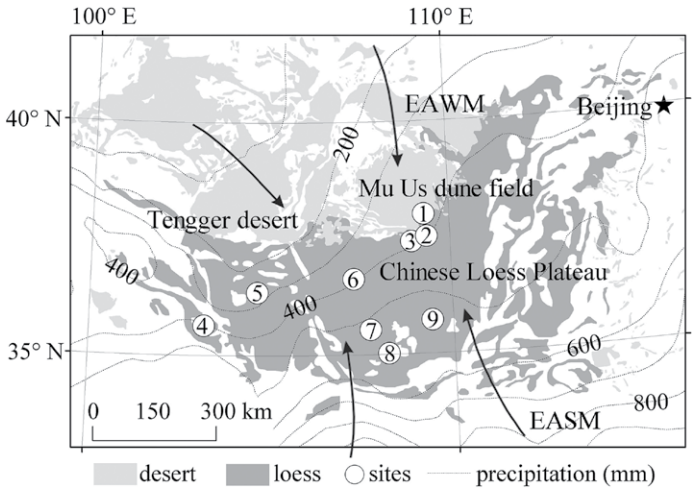

Figure 1. Chinese Loess Plateau, with East Asian winter monsoon (EAWM) and summer monsoon (EASM) indicated by arrows. Study sites: 1—LP19; 2—LP12; 3—LP03; 4—Yuanbao; 5—Jingyuan; 6—Beiguoyuan; 7—Xifeng; 8—Luochuan; 9—Xunyi.

*E-mail: zhiweixu@nju.edu.cn

CITATION: Xu, Z., Stevens, T., Yi, S., Mason, J.A., and Lu, H., 2018, Seesaw pattern in dust accumulation on the Chinese Loess Plateau forced by late glacial shifts in the East Asian monsoon: Geology, v. 46, p. 871–874, https://doi.org/10.1130/G45105.1

grains with grain sizes of 63–90/90–150 µm were measured using a Risø TL/OSL-DA-20C/D reader fitted with blue-green diodes (λ = 470 ± 30 nm) and infrared light-emitting diodes (IR-LEDs) emitting at 880 ± 80 nm. Single-aliquot regenerative-dose OSL dating methods were applied (Wintle and Murray, 2006). Concentrations of U, Th, and K were measured by neutron activation analysis to determine the dose rate. The new ages are illustrated in Figure 2 and listed in the GSA Data Repository[1]. Samples from six other sites with existing quartz OSL ages were synthesized and analyzed, including Beiguoyuan, Xifeng, Luochuan, and Xunyi, which were published in our previous studies (Stevens et al., 2006, 2008; Lu et al., 2013), and Jingyuan (Sun et al., 2012) and Yuanbao (Lai and Wintle, 2006). These sites were chosen because they are classic loess sites reported with high-sampling-resolution ages, almost completely spanning the past 20 k.y. Similar procedures were followed for quartz OSL dating, though the coarse silt fraction was in some cases used in order to date the major grain-size component. Beiguoyuan, Jingyuan, and Yuanbao, from the northern/northwestern CLP, are proximal to the desert and are classified as N (NW) sites. Xifeng, Luochuan, and Xunyi are distal from the southern/southeastern CLP and are referred to as S (SE) sites.

Sedimentation rate (SR, m/k.y.) and mass accumulation rate (MAR, g/cm^2/k.y.) have been calculated by several methods (Kang et al., 2015; Albani et al., 2015; Újvári et al., 2017; Perić et al., 2018). Since luminescence sampling resolution differs among the nine sites, we applied a simple piecewise linear regression model to calculate the SR and MAR at a coarse resolution. The age for each sample of the three new records was derived based on linear age-depth models. To emphasize how the spatial pattern of dust accumulation varied between major paleoclimate phases, we calculated MARs for 5000 yr time windows, 20–15 ka, 15–10 ka, and 10–5 ka, roughly representing the mean dust conditions during glacial, deglacial, and postglacial periods, respectively. MAR was computed from SR multiplied by an estimate of 1.48 g/cm^3 for the mean dry bulk density of the sediment (Kang et al., 2015).

RESULTS AND DISCUSSION

Deglacial and Postglacial Dust Accumulation at the Desert Margin

Samples LP03, LP12, and LP19 were composed of loess, paleosol, and a buried sand layer (Fig. 2). This eolian sand layer, of 1–3 m thickness, is widespread in the transition zone between the desert and the CLP. Mean grain size of the sand was mostly >100 µm. The loess accumulated above the sand was 1–2 m thick, with a mean grain size of 60–90 µm, which is substantially coarser than typical loess in the central CLP. The paleosols overlying the loess were ~1 m thick and had similar grain size as the loess.

The OSL age of the sand was ca. 20 ka in LP03, and ca. 15 ka in samples LP12 and LP19. This is consistent with the previous finding that the Mu Us dune field was expanding into the CLP during the Last Glacial Maximum (LGM) and Heinrich event 1 (H1; Xu et al., 2015). The ages of the loess overlying the sands were between 15 and 10 ka, indicating that dust began to accumulate at the desert margin following stabilization of the dunes. The desert boundary shifted toward the north/northwest after ca. 15 ka, corresponding to the termination of H1 and the onset of the Bølling-Allerød interstadial (Wang et al., 2001; Andrews and Voelker, 2018). The paleosols with ages younger than 10 ka were developed during the Holocene.

The deglacial loess covering the LGM sand dunes is found not only at the desert-marginal sites near the Mu Us dune field, but also near the southern margin of Tengger Desert (Peng et al., 2016). In Qinwangchuan Basin, south of the Tengger Desert, large dunes are buried by loess that accumulated after ca. 15 ka (Long et al., 2016). Thus, it is inferred that rapid dust accumulation has been fairly extensive in the desert-marginal regions of northern China after the end of H1.

Seesaw in Dust Accumulation on the CLP

By comparing the new results with previously studied sites, it is clear that dust accumulation over the CLP varied both spatially and temporally since the last glaciation (Figs. 3 and 4). At the desert-marginal sites, MAR reached 50 g/cm^2/k.y. during 15–10 ka and remained as high as 30 g/cm^2/k.y. during 10–5 ka (Fig. 4). Interestingly, the N (NW) sites showed a significant reduction in SR after ca. 15 ka (Fig. 3), and their MARs decreased from ~100 g/cm^2/k.y. to less than 25 g/cm^2/k.y. The S (SE) sites showed extremely low MAR during 15–10 ka, whereas they were higher before and after that time. Clear gaps and scattering in ages were observed within the deglacial period at the S (SE) sites (Fig. 3), in spite of the close and uniform spacing of the dated samples.

The reduction in loess SR at the N (NW) sites after 15 ka occurred simultaneously with rapid accumulation at the desert-marginal sites. At the S (SE) sites, deglacial age loess dated between 15 and 10 ka is quite rare. The spatial variations between these sites indicate a clear seesaw pattern before and after 15 ka: During the LGM and H1, the margins of the CLP experienced intensive erosion, while strong dust accumulation occurred in the main CLP; since the last deglaciation, dust accumulated

[1]GSA Data Repository item 2018320, dosimetric and chronologic data, is available online at http://www.geosociety.org/datarepository/2018/ or on request from editing@geosociety.org.

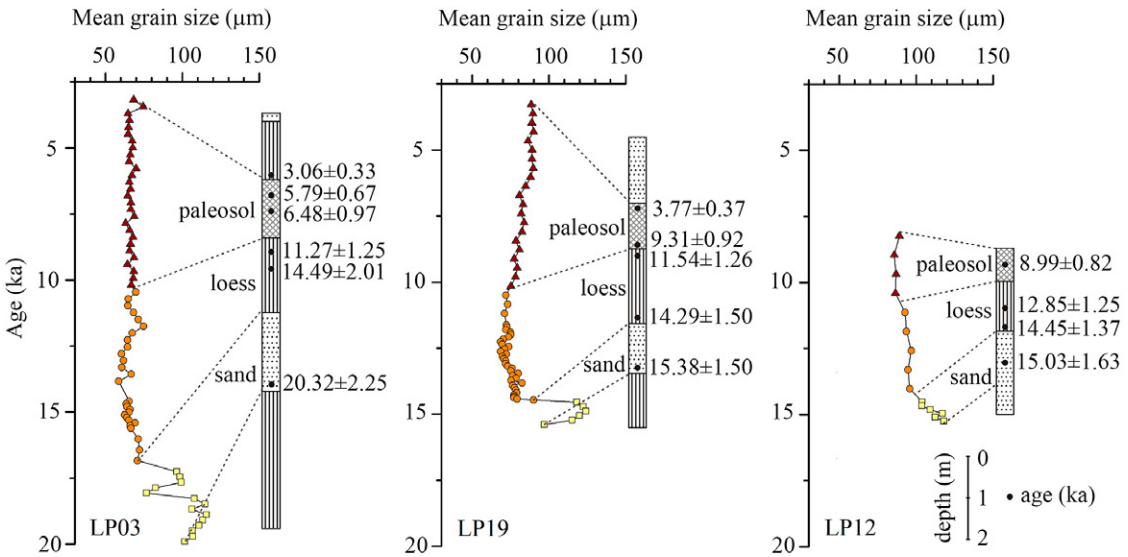

Figure 2. Stratigraphy, age, and mean grain size of three desert-marginal records (LP03, LP12, and LP19). Age for each sample was derived from linear age-depth model established for each site.

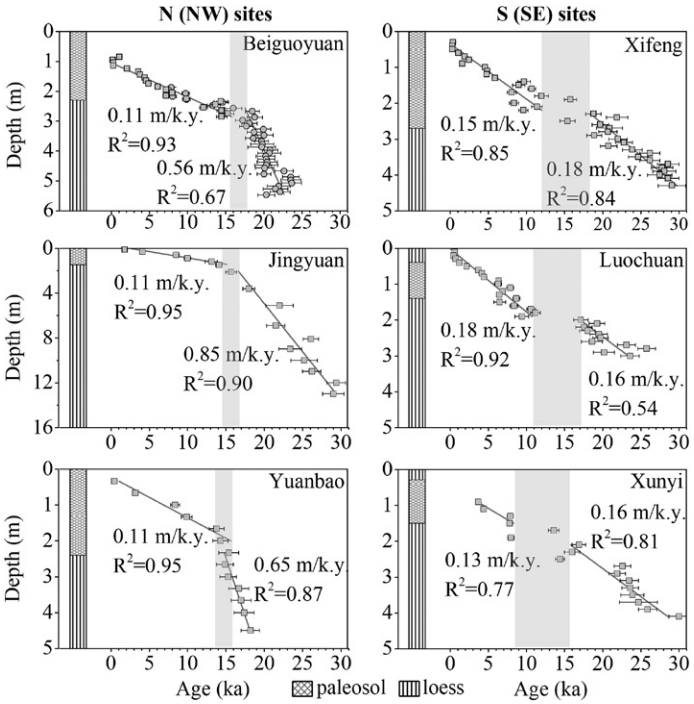

Figure 3. Optically stimulated luminescence (OSL) ages and sedimentation rate (SR) of N (NW) and S (SE) sites on Chinese Loess Plateau (Lai and Wintle, 2006; Sun et al., 2012; Stevens et al., 2006, 2008; Lu et al., 2013). Gray bar shown in N (NW) sites marks shift in loess SR after ca. 15 ka. Gray bar in S (SE) sites indicates gaps and scattering in ages. Beiguoyuan site is composed of two nearby sections (for details, see Stevens et al., 2006).

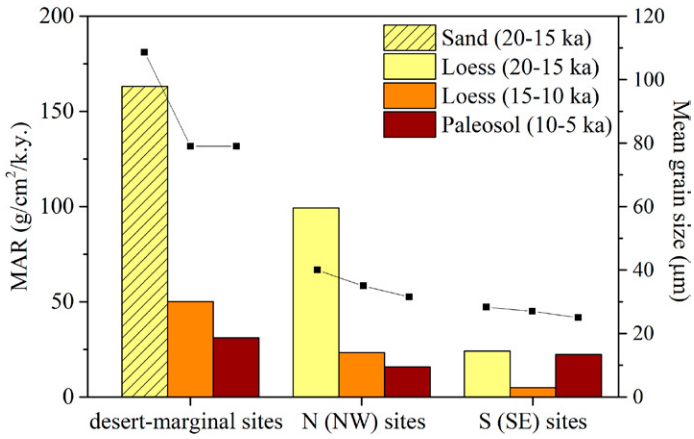

Figure 4. Comparison of mass accumulation rates (MARs, bar) and mean grain size (plot) between different settings during periods: 20–15 ka, 15–10 ka, and 10–5 ka.

rapidly at the desert margin, while loess SR was reduced in the main CLP. Importantly, although these different sites experienced different "events" in loess sedimentation, these events show synchronicity and probably can be linked in terms of overarching cause.

Links to East Asian Monsoon Dynamics

Loess sedimentation is dominated by primary dust accumulation and postdepositional processes that affect dust preservation. Primary dust accumulation is related to the availability of dust in the atmosphere, the frequency and magnitude of dust-transporting winds, and dust-trapping conditions (Pye and Tsoar, 1987). During both glacial and interglacial times, the large drylands located to the north and northwest of the CLP could emit dust effectively (Nie et al., 2015). The strength of dust-transporting winds on the CLP is closely linked to the East Asian winter monsoon (EAWM), while the East Asian summer monsoon (EASM) transports moisture to the CLP from the southeast and influences vegetation growth and postdepositional processes including erosion, weathering, and pedogenesis (Liu and Ding, 1998; Maher, 2016).

Many independent reconstructions indicate a weakened EAWM since the last deglaciation (e.g., Steinke et al., 2011; Sun et al., 2012). The declining EAWM wind strength can be inferred from records of loess grain size, which decreases after 15 ka. The decreasing dust flux associated with a weakened EAWM is also observed in other downwind dust-depositional regions, including Lake Biwa of Japan (Xiao et al., 1997) and the northwest Pacific Ocean (Hovan et al., 1991). Meanwhile, the EASM rain belt has migrated northwestward since the LGM (Yang et al., 2015). The general increase in EASM intensity after the termination of H1 has been identified in many types of records, even if the exact timing is still debated (e.g., Wang et al., 2001; Lu et al., 2013; Chen et al., 2015).

The seesaw in loess sedimentation since the last deglaciation is probably related to the shift in EAWM and EASM circulation. The coarse desert-marginal loess accumulated wherever there was a significant reduction in wind speed and/or suitable trapping conditions, i.e., vegetated surfaces (Pye and Tsoar, 1987). The enhanced EASM after 15 ka would have promoted the growth of vegetation, which, along with weakened winds, enhanced sandy loess accumulation near the desert margin. However, at the N (NW) sites, dust accumulation was reduced due to the weakened EAWM. The retreat of desert margin increased the distance to dust sources, which may also explain the decreasing loess grain size and MAR at downwind sites (Nugteren and Vandenberghe, 2004). Mass wasting and erosion induced by more EASM precipitation and surface runoff could have reduced loess preservation, thus playing a secondary role in reducing net accumulation at these sites (Lu et al., 2006; Stevens et al., 2006).

The low dust MAR during 15–10 ka at the S (SE) sites was very likely caused by increased EASM precipitation as well, through its effect on postdepositional disturbance (Lu et al., 2006). Bioturbation during pedogenesis can homogenize sediments and reset their OSL signals through light exposure; the measured OSL age of the disturbed loess could then be offset relative to time of deposition and fall within the time of subsequent soil formation (Stevens et al., 2006, 2008, 2016; Sun et al., 2010; Kang et al., 2013). The considerable scatter of ages at the base of Holocene soils (Fig. 3) supports this idea. Reworking of deglacial loess at the S (SE) sites by Holocene soil formation may account for the high apparent MARs during 10–5 ka, almost equal to that of the glacial period and even exceeding those of the N (NW) sites.

CONCLUSIONS AND IMPLICATIONS

A clear seesaw pattern in dust accumulation is indicated by stronger accumulation at the desert margin and reduced accumulation/less preservation in the main CLP after ca. 15 ka. Changes in loess sedimentation in different geographic settings coincided in time after the termination of H1, in response to decreased EAWM winds and increased EASM precipitation. This implies that dust activity and deposition on the CLP are sensitive to subglacial-interglacial monsoon climate change. However, loess sedimentation exhibits strong spatial variability and should be viewed as a dynamic process involving episodic deposition and postdepositional alteration, especially when utilizing loess deposits as paleoclimate archives.

Our study has one more important implication. Kapp et al. (2015) suggested that the CLP might have previously extended farther north and west of its modern margin. Our study implies that the boundary between the Mu Us dune field and the CLP shifted during glacial-interglacial cycles, because dust was trapped at the desert margin when it became vegetated during the humid and warm interglacial period. The dust depositional center also moved to the north and west during deglaciation, as indicated

by stronger dust accumulation at the desert margin than in the main CLP. During the glacial period, however, this region was dominated by the extension of sand dunes (Xu et al., 2015), and the loess that was accumulated during prior glacial or interglacial periods was subject to wind erosion (Kapp et al., 2015; Stevens et al., 2018). Therefore, the desert margin, as well as the northern CLP, serves as a transition zone that accumulates dust during interglacials and emits dust during glacials. This provides an important dust transport and recycling pathway that carries dust from the north/northwest to the south/southeast over glacial-interglacial cycles.

ACKNOWLEDGMENTS

This study was supported by the National Key R&D Program of China (grant 2016YFA0600503), the National Natural Science Foundation of China (grants 41501208 and 41690111), and a research grant from Nanjing University (020814380089).

REFERENCES CITED

Albani, S., et al., 2015, Twelve thousand years of dust: The Holocene global dust cycle constrained by natural archives: Climate of the Past, v. 11, p. 869–903, https://doi.org/10.5194/cp-11-869-2015.

Andrews, J.T., and Voelker, A.H.L., 2018, "Heinrich events" (& sediments): A history of terminology and recommendations for future usage: Quaternary Science Reviews, v. 187, p. 31–40, https://doi.org/10.1016/j.quascirev.2018.03.017.

Chen, F., et al., 2015, East Asian summer monsoon precipitation variability since the last deglaciation: Scientific Reports, v. 5, p. 11186, https://doi.org/10.1038/srep11186.

Hovan, S.A., Rea, D.K., and Pisias, N.G., 1991, Late Pleistocene continental climate and oceanic variability recorded in northwest Pacific sediments: Paleoceanography, v. 6, p. 349–370, https://doi.org/10.1029/91PA00559.

Kang, S., Wang, X., and Lu, Y., 2013, Quartz OSL chronology and dust accumulation rate changes since the Last Glacial at Weinan on the southeastern Chinese Loess Plateau: Boreas, v. 42, p. 815–829.

Kang, S., Roberts, H.M., Wang, X., An, Z., and Wang, M., 2015, Mass accumulation rate changes in Chinese loess during MIS 2, and asynchrony with records from Greenland ice cores and North Pacific Ocean sediments during the Last Glacial Maximum: Aeolian Research, v. 19, p. 251–258, https://doi.org/10.1016/j.aeolia.2015.05.005.

Kapp, P., Pullen, A., Pelletier, J.D., Russell, J., Goodman, P., and Cai, F., 2015, From dust to dust: Quaternary wind erosion of the Mu Us Desert and Loess Plateau, China: Geology, v. 43, p. 835–838, https://doi.org/10.1130/G36724.1.

Lai, Z., and Wintle, A.G., 2006, Locating the boundary between the Pleistocene and the Holocene in Chinese loess using luminescence: The Holocene, v. 16, p. 893–899, https://doi.org/10.1191/0959683606hol980rr.

Licht, A., Pullen, A., Kapp, P., Abell, J., and Giesler, N., 2016, Eolian cannibalism: Reworked loess and fluvial sediment as the main sources of the Chinese Loess Plateau: Geological Society of America Bulletin, v. 128, p. 944–956, https://doi.org/10.1130/B31375.1.

Liu, T.S., and Ding, Z.L., 1998, Chinese loess and the palaeomonsoon: Annual Review of Earth and Planetary Sciences, v. 26, p. 111–145, https://doi.org/10.1146/annurev.earth.26.1.111.

Long, H., Fuchs, M., Yang, L., and Cheng, H., 2016, Abrupt sand-dune accumulation at the northeastern margin of the Tibetan Plateau challenges the wet MIS3a inferred from numerous lake-highstands: Scientific Reports, v. 6, p. 25820, https://doi.org/10.1038/srep25820.

Lu, H., Stevens, T., Yi, S., and Sun, X., 2006, An erosional hiatus in Chinese loess sequences revealed by closely spaced optical dating: Chinese Science Bulletin, v. 51, p. 2253–2259, https://doi.org/10.1007/s11434-006-2097-x.

Lu, H., et al., 2013, Variation of East Asian monsoon precipitation during the past 21 k.y. and potential CO_2 forcing: Geology, v. 41, p. 1023–1026, https://doi.org/10.1130/G34488.1.

Maher, B.A., 2016, Palaeoclimatic records of the loess/palaeosol sequences of the Chinese Loess Plateau: Quaternary Science Reviews, v. 154, p. 23–84, https://doi.org/10.1016/j.quascirev.2016.08.004.

Nie, J., et al., 2015, Loess plateau storage of northeastern Tibetan Plateau–derived Yellow River sediment: Nature Communications, v. 6, p. 8511, https://doi.org/10.1038/ncomms9511.

Nugteren, G., and Vandenberghe, J., 2004, Spatial climatic variability on the Central Loess Plateau (China) as recorded by grain size for the last 250 kyr: Global and Planetary Change, v. 41, p. 185–206, https://doi.org/10.1016/j.gloplacha.2004.01.005.

Peng, J., Dong, Z., Han, F., and Gao, L., 2016, Aeolian activity in the south margin of the Tengger Desert in northern China since the Late Glacial period revealed by luminescence chronology: Palaeogeography, Palaeoclimatology, Palaeoecology, v. 457, p. 330–341, https://doi.org/10.1016/j.palaeo.2016.06.028.

Perić, Z., et al., 2018, Quartz OSL dating of late Quaternary Chinese and Serbian loess: A cross Eurasian comparison of dust mass accumulation rates: Quaternary International, https://doi.org/10.1016/j.quaint.2018.01.010 (in press).

Pye, K., and Tsoar, H., 1987, The mechanics and geological implications of dust transport and deposition in deserts with particular reference to loess formation and dune sand diagenesis in the northern Negev, Israel, *in* Frostick, L.E., et al., eds., Desert Sediments: Ancient and Modern: Geological Society of London Special Publication 35, p. 139–156, https://doi.org/10.1144/GSL.SP.1987.035.01.10.

Schaetzl, R.J., et al., 2018, Approaches and challenges to the study of loess—Introduction to the LoessFest Special Issue: Quaternary Research, v. 89, p. 563–618, https://doi.org/10.1017/qua.2018.15.

Steinke, S., Glatz, C., Mohtadi, M., Groeneveld, J., Li, Q., and Jian, Z., 2011, Past dynamics of the East Asian monsoon: No inverse behaviour between the summer and winter monsoon during the Holocene: Global and Planetary Change, v. 78, p. 170–177, https://doi.org/10.1016/j.gloplacha.2011.06.006.

Stevens, T., Armitage, S.J., Lu, H., and Thomas, D.S.G., 2006, Sedimentation and diagenesis of Chinese loess: Implications for the preservation of continuous, high-resolution climate records: Geology, v. 34, p. 849–852, https://doi.org/10.1130/G22472.1.

Stevens, T., Lu, H., Thomas, D.S.G., and Armitage, S.J., 2008, Optical dating of abrupt shifts in the late Pleistocene East Asian monsoon: Geology, v. 36, p. 415–418, https://doi.org/10.1130/G24524A.1.

Stevens, T., Buylaert, J.P., Lu, H., Thiel, C., Murray, A., Frechen, M., Yi, S., and Zeng, L., 2016, Mass accumulation rate and monsoon records from Xifeng, Chinese Loess Plateau, based on a luminescence age model: Journal of Quaternary Science, v. 31, p. 391–405, https://doi.org/10.1002/jqs.2848.

Stevens, T., Buylaert, J.P., Thiel, C., Újvári, G., Yi, S., Murray, A.S., Frechen, M., and Lu, H., 2018, Ice-volume-forced erosion of the Chinese Loess Plateau global Quaternary stratotype site: Nature Communications, v. 9, p. 983, https://doi.org/10.1038/s41467-018-03329-2.

Sun, Y., Wang, X., Liu, Q., and Clemens, S.C., 2010, Impacts of post-depositional processes on rapid monsoon signals recorded by the last glacial loess deposits of northern China: Earth and Planetary Science Letters, v. 289, p. 171–179, https://doi.org/10.1016/j.epsl.2009.10.038.

Sun, Y., Clemens, S.C., Morrill, C., Lin, X., Wang, X., and An, Z., 2012, Influence of Atlantic meridional overturning circulation on the East Asian winter monsoon: Nature Geoscience, v. 5, p. 50–54.

Újvári, G., et al., 2017, Coupled European and Greenland last glacial dust activity driven by North Atlantic climate: Proceedings of the National Academy of Sciences of the United States of America, v. 114, E10632, https://doi.org/10.1073/pnas.1712651114.

Wang, Y., Cheng, H., Edwards, R.L., An, Z.S., Wu, J.Y., Shen, C.C., and Dorale, J.A., 2001, A high-resolution absolute-dated late Pleistocene monsoon record from Hulu Cave, China: Science, v. 294, p. 2345–2348, https://doi.org/10.1126/science.1064618.

Wintle, A.G., and Murray, A.S., 2006, A review of quartz optically stimulated luminescence characteristics and their relevance in single-aliquot regeneration dating protocols: Radiation Measurements, v. 41, p. 369–391, https://doi.org/10.1016/j.radmeas.2005.11.001.

Xiao, J., Inouchi, Y., Kumai, H., Yoshikawa, S., Kondo, Y., Liu, T., and An, Z., 1997, Eolian quartz flux to Lake Biwa, central Japan, over the past 145,000 years: Quaternary Research, v. 48, p. 48–57, https://doi.org/10.1006/qres.1997.1893.

Xu, Z., Lu, H., Yi, S., Vandenberghe, J., Mason, J.A., Zhou, Y., and Wang, X., 2015, Climate-driven changes to dune activity during the Last Glacial Maximum and deglaciation in the Mu Us dune field, north-central China: Earth and Planetary Science Letters, v. 427, p. 149–159, https://doi.org/10.1016/j.epsl.2015.07.002.

Yang, S., Ding, Z., Li, Y., Wang, X., Jiang, W., and Huang, X., 2015, Warming-induced northwestward migration of the East Asian monsoon rain belt from the Last Glacial Maximum to the mid-Holocene: Proceedings of the National Academy of Sciences of the United States of America, v. 112, p. 13,178–13,183, https://doi.org/10.1073/pnas.1504688112.

Printed in USA